American Journal of Pathology, Vol. 166, No. 3, March 2005

Musculoskeletal Pathology

A Cyclosporine-Sensitive Psoriasis-Like Disease Produced in Tie2 Transgenic Mice

Daniel Voskas,*† Nina Jones,† Paul Van Slyke,*† Celina Sturk,*† Wing Chang,‡¶ Alex Haninec,*† Yael Olya Babichev,† Jennifer Tran,† Zubin Master,*† Stephen Chen,*† Nicole Ward,§ Maribelle Cruz,† Jamie Jones,† Robert S. Kerbel,*† Serge Jothy,‡ Lina Dagnino,‡¶ Jack Arbiser,‖ Giannoula Klement,** and Daniel J. Dumont*†††

From the Department of Medical Biophysics, University of Toronto, Toronto, Ontario, Canada; the Division of Molecular and Cellular Biology,† Sunnybrook and Women's Research Institute, Toronto, Ontario, Canada; the Toronto-Sunnybrook Regional Cancer Centre,†† Toronto, Ontario, Canada; the Department of Anatomy,§ Case Western University, Cleveland, Ohio; the Department of Laboratory Medicine and Pathobiology,‡ St. Michael's Hospital, Toronto, Ontario, Canada; the Departments of Physiology/Pharmacology and Paediatrics,¶ the University of Western Ontario, London, Ontario, Canada; the Child Health Research Institute and Lawson Health Research Institute,‡ London, Ontario, Canada; the Department of Dermatology,‖ Emory University School of Medicine, Atlanta, Georgia; and Department of Pediatric Oncology,** Dana-Farber Cancer Institute, Boston, Massachusetts*

Psoriasis is a common, persistent skin disorder characterized by recurrent erythematous lesions thought to arise as a result of inflammatory cell infiltration and activation of keratinocyte proliferation. Unscheduled angiogenic growth has also been proposed to mediate the pathogenesis of psoriasis although the cellular and molecular basis for this response remains unclear. Recently, a role for the angiopoietin signaling system in psoriasis has been suggested by studies that demonstrate an up-regulation of the tyrosine kinase receptor Tie2 (also known as Tek) as well as angiopoietin-1 and angiopoietin-2 in human psoriatic lesions. To examine temporal expression of Tie2, we have developed a binary transgenic approach whereby expression of Tie2 can be conditionally regulated by the presence of tetracycline analogs in double-transgenic mice. A psoriasis-like phenotype developed in double-transgenic animals within 5 days of birth and persisted throughout adulthood. The skin of affected mice exhibited many cardinal features of human psoriasis including epidermal hyperplasia, inflammatory cell accumulation, and altered dermal angiogenesis. These skin abnormalities resolved completely with tetracycline-mediated suppression of transgene expression, thereby illustrating a complete dependence on Tie2 signaling for disease maintenance and progression. Furthermore, the skin lesions in double-transgenic mice markedly improved after administration of the immunosuppressive antipsoriatic agent cyclosporine, thus demonstrating the clinical significance of this new model. ***(Am J Pathol 2005, 166:843–855)***

Development of the cardiovascular system involves the coordinated interactions between numerous growth factors and receptors that selectively regulate the vascular endothelium. The angiopoietins bind the tyrosine kinase with immunoglobulin and epidermal growth factor homology domains 2 (Tie2) receptor [also known as the tunica interna endothelial cell kinase (Tek) receptor] and lead to the context-specific activation of the receptor and downstream signal transduction pathways that control angiogenic remodeling.[1–4] The effect of the angiopoietins on the microcirculation is somewhat less clear;[5] however, Tie2 is required for vessel maintenance[6,7] and it is currently believed that temporally regulated expression of angiopoietin-2 (Ang2) in concert with vascular endothelial growth factor (Vegf) may antagonize the constitutively stabilizing function of angiopoietin-1 (Ang1) to facilitate vascular destabilization and vessel sprouting.[4]

Supported by the Canadian Institute for Health Research, the National Institutes of Health (grant HL63224-01), and the Heart and Stroke Society of Canada (studentships to D.V. and C.S., and fellowship to Y.O.B.).

Accepted for publication November 24, 2004.

The authors declare no competing financial interests.

D.J.D. is a Canadian Institute for Health Research scientist and is a member of the Heart and Stroke/Richard Lewar Centre of Excellence, University of Toronto, Canada.

Address reprint requests to Daniel J. Dumont, Sunnybrook and Women's Research Institute, 2075 Bayview Ave., Research Building, S-227, Toronto, Ontario, Canada, M4N 3M5. E-mail: dan.dumont@swri.ca.

The identification of a unique family of natural agonists and competitive context-dependent antagonists implies exquisite control over Tie2-mediated vascular plasticity and perturbations in Tie2-regulated angiogenesis have been documented in a number of skin lesions. Mice overexpressing Ang1 in the skin develop highly branched dermal blood vessels that are larger than those seen in normal skin.[8] Dilated blood vessels with similar morphology have also been observed in human patients with venous malformations arising as a result of gain of function mutations in Tie2.[9] Furthermore, expression of Tie2 and the angiopoietins has been shown to be up-regulated in human psoriasis.[10] Psoriasis is a chronic inflammatory skin disorder characterized by epidermal hyperplasia, altered keratinocyte differentiation, and expansion of the dermal vasculature. Abnormalities in the microvasculature occur very early during the progression of psoriasis and are required for disease maintenance. In psoriatic lesions, affected microvessels of the papillary dermis below the epidermal surface display numerous distinctive morphological changes such as dilatation and tortuosity in addition to increased permeability.[11]

Here we demonstrate that conditional overexpression of Tie2 from its minimal promoter drives expression in endothelial cells and keratinocytes resulting in a reversible skin disorder resembling human psoriasis. Transgenic mice display an increased number of large and tortuous capillaries in the dermis accompanied by an inflammatory infiltrate and an overlying hyperplastic epidermis. Onset, progression, and maintenance of the psoriasiform phenotype rely on the continued expression of the Tie2 transgene. Moreover, the skin phenotype can be morphologically and histologically resolved on immunosuppressive cyclosporine A (CsA) treatment.

Materials and Methods

Generation, Genotyping, and Doxycycline/CsA Treatment of Transgenic Mice

Construction of the driver transgene, pTek-*tTA*, and the responder transgenes, pTet^{OS}-*Tek* and pTet^{OS}-*nlsLacZ*, have been described previously.[7,12] All transgenic lines were maintained and genotyped as previously described.[7,12] The pTek-*tTA* driver and pTet^{OS}-*nlsLacZ* responder transgenes were amplified using primers described in Sarao and Dumont[12] and the pTet^{OS}-*Tek* responder transgene was amplified using primers described in Jones and colleagues.[7] To repress pTet^{OS}-*Tek* responder transgene expression, 200 μg/ml of doxycycline (Sigma Chemical Co., St. Louis, MO) supplemented with 5% sucrose was added to the drinking water of double-transgenic (DT) and normal wild-type (WT) mice. Alternatively, DT and normal mice were orally fed every third day with 80 mg/kg of CsA (Novartis Pharmaceuticals Canada Inc, Dorval, Quebec, Canada), every day with 10 mg/kg of doxycycline or every day with saline alone for a period of 12 days. Males were housed with a single female for 14 to 20 days and then separated into individual cages. CD1 mice (an outbred mouse line) were maintained in a barrier-free facility that was exposed to epizootic diarrhea of infant mice and mouse hepatitis virus. After an extensive burnout procedure, subsequent testing of sentinels revealed an absence of viral antigens. Furthermore, the fertility of DT and WT animals was unaffected. All adult mice used in these studies were 4 to 6 months old and unless otherwise specified, mice from each age group (neonates or adults) were generated, treated, and biochemically or immunohistochemically examined at least in triplicate ($n = 3$).

Cell Lines and Culture

The isolation of primary mouse (pm) and primary human (ph) keratinocyte cells (KCs) used in this work have been previously described.[13,14] pmKCs were treated with 1 mmol/L $CaCl_2$ to induce differentiation.[13] Mouse endothelioma cells were derived by infecting primary cells from embryonic day 9.5 litters with a retrovirus coding for the Polyoma virus middle T antigen[15] and maintained in Dulbecco's modified Eagle's medium (Invitrogen, Carlsbad, CA) supplemented with 10% fetal bovine serum (Sigma), 5 μmol/L β-mercaptoethanol (Sigma), 1 mmol/L sodium pyruvate, 1% nonessential amino acids, 1% penicillin-streptomycin, and 1% glutamine (Invitrogen) and human umbilical vein endothelial cells were purchased from the American Type Culture Collection, Rockville, MD, and maintained in F-12 nutrient mixture (Invitrogen) supplemented with 5 ng/ml of basic fibroblast growth factor, 10 ng/ml of epidermal growth factor, 10 ng/ml of Vegf (R&D Systems, Minneapolis, MN), 10% fetal bovine serum, 0.1 mg/ml of heparin (ICN Biomedicals, Irvine, CA), 1% penicillin-streptomycin, and 1% glutamine. MCF-7 epithelial cells were maintained in improved modified Eagle's medium (Invitrogen) supplemented with 10% fetal bovine serum, 1× penicillin-streptomycin, and 1× glutamine. All cultures were maintained on plastic (Nunc, Naperville, IL) at 37°C in a humidified 5% CO_2 atmosphere. Human umbilical vein endothelial cells were maintained on plates coated with 2% gelatin (Sigma).

Gene Expression Analysis

Total RNA was isolated using Trizol reagent (Life Technologies, Inc., Grand Island, NY) and reverse transcriptase (RT) for polymerase chain reaction (PCR) was performed using the First-Strand cDNA synthesis kit (Clontech, Palo Alto, CA). PCR was performed by amplifying cDNA templates that were undiluted, diluted 1 in 10, 1 in 100, or 1 in 1000. Mouse and human vascular endothelial (*Ve)-cadherin* and *βActin* primers have been described previously.[16,17] *Tie2* primers were designed to amplify mouse and human sequences (327-bp regions) and cross intron/exon boundaries. *Tie2* forward primer 5′-GAT TTT GGA TTG TCC CGA GGT CAA G-3′ and *Tie2* reverse primer 5′-CAC CAA TAT CTG GGC AAA TGA TGG-3′. The pTet^{OS}-*Tek* template was detected using primers described in Jones and colleagues.[7]

LacZ Expression Analysis

Mouse skin tissue was fixed in 4% paraformaldehyde (pH 7.4) (Fisher Scientific, Pittsburgh, PA) for 4 hours at room temperature, cryoembedded in optimal cutting temperature (OCT) compound (VWR International, Mississauga, Ontario, Canada), sectioned (8 μm) on SuperFrost glass slides (Fisher Scientific), and processed and stained for nlsLacZ expression as previously described in Dumont and colleagues.[1]

Immunoprecipitation and Western Analysis

Frozen tissues were homogenized in phospholipase Cγ (PLCγ) lysis buffer and equivalent amounts of cleared extracts were precipitated with 1 μg of anti-Tie2 (C-20; Santa Cruz Biotechnology, Santa Cruz, CA) or anti-DokR antibodies, as described previously.[18] Western blotting was performed as described previously.[18] Commercially available antibodies used were as follows: polyclonal anti-phospho-Tie2 (Calbiochem, La Jolla, CA), monoclonal anti-phosphotyrosine 4G10 (Upstate Biotechnology, Lake Placid, NY), polyclonal anti-phospho-Akt (New England Biolabs, Beverly, MA), polyclonal anti-Ang1 (Chemicon, Temecula, CA), polyclonal anti-Vegf (A-20; Santa Cruz Biotechnology), and monoclonal anti-Actin (A-40; Sigma). Monoclonal anti-Tie2 and polyclonal anti-DokR have been described elsewhere.[18] Densitometry was performed using ImageQuant software (Molecular Dynamics, Eugene, OR).

Vegf Enzyme-Linked Immunosorbent Assay

Fresh tissues were homogenized in radioimmune precipitation buffer (RIPA) lysis buffer[19] and extracts were centrifuged at 9,300 ref for 10 minutes. Total protein was quantified using Bradford reagent and Vegf was quantified as described in the Quantikine M kit (R&D Systems). Plates were read using a Benchmark Plus microplate spectrophotometer (Bio-Rad, Hercules, CA).

Gelatin Zymography

Fresh tissues were homogenized in 500 mmol/L Tris-HCl, pH7.6, 200 mmol/L NaCl, 10 mmol/L $CaCl_2$, and 1% Triton X-100 and equal amounts of cleared lysate were loaded onto a 12.5% sodium dodecyl sulfate-polyacrylamide gel co-polymerized with 1 mg/ml of gelatin. Electrophoresis was performed under nonreducing conditions at 100 V for 4 hours. Gels were washed overnight in 2.5% Triton X-100 to remove sodium dodecyl sulfate and were then incubated in substrate buffer (50 mmol/L Tris-HCl, pH 8.8, 5 mmol/L $CaCl_2$) for 40 hours at 37°C. Gels were then stained with 0.5% Coomassie blue in 30% methanol/10% acetic acid for 2 hours at room temperature and destained in 50% methanol/10% acetic acid. The presence of metalloproteinases was indicated by unstained proteolytic zones in the gel. Densitometry was performed as described above.

Morphological and Histological Analysis

Gross pathology screens were performed by the Centre for Modeling Human Disease at the Samuel Lunenfeld Research Institute (*www.cmhd.ca*). Mice were photographed using a Cybershot digital camera (Sony). Skin tissue was isolated from approximately the same anatomical site on the back of all DT and normal mice. Skin tissue was fixed in 4% paraformaldehyde (pH 7.4) solution for 4 hours at room temperature, embedded in paraffin, sectioned (6 μm) on SuperFrost glass slides, and processed and stained for hematoxylin and eosin (H&E) or toluidine blue using standard techniques. Slides were analyzed on a Zeiss Axioplan 2 light microscope (Carl Zeiss, Thornwood, NY) and photos were processed using Adobe Photoshop v6.0 (Adobe Systems, San Jose, CA).

Immunohistochemical Analysis

Mouse skin tissue was fixed in Histochoice (Amresco, Solou, Ohio) for 4 hours at room temperature, cryoembedded in OCT compound, and sectioned (8 μm) on SuperFrost glass slides. For immunohistochemistry, anti-Panec (rat; Pharmingen, La Jolla, CA), anti-Pecam1 (rat; Pharmingen), anti-SMA (mouse; DAKO, Carpinteria, CA), and anti-CD3 (hamster; Pharmingen) primary antibodies were detected using biotinylated secondary antibodies as described in the Vectastain Elite ABC kit (Vector Laboratories, Burlingame, CA). Slides were processed and counterstained with methyl green using standard techniques. Slides were analyzed and photos were processed as above.

Lectin and Immunofluorescent Analysis

Mice were anesthetized and injected intravenously via the tail vein with 100 μg of fluorescein isothiocyanate-labeled *Lycopersicon esculentum* (Vector Laboratories) and perfused with 0.5% glutaraldehyde and 1% paraformaldehyde (pH 7.4) at 120 to 140 mmHg. Mouse skin tissues were cryoembedded in OCT compound and sectioned (100 μm) on SuperFrost glass slides. For confocal analysis, a Cy3-labeled anti-SMA primary antibody (goat; Sigma) was used and anti-Panec (rat; Pharmingen) or anti-Pecam1 (rat; Pharmingen) primary antibodies were detected with Cy3-conjugated secondary antibodies (Jackson Laboratories, Bar Harbor, ME) and anti-Tie2 (rat; Tek4) antibodies[20] were detected with fluorescein isothiocyanate-conjugated secondary antibodies (Jackson Laboratories). Slides were analyzed on a Zeiss Axiovert 100 M confocal microscope (Carl Zeiss) for three-dimensional image reconstruction and photos were processed as above.

Quantitative Analysis of Epidermal Thickness and Blood Vessel Morphology

Epidermal thickness and blood vessel area density, number, and diameter were measured in sections from equivalent areas of DT and WT adult skin stained with H&E or

lectin using Zeiss LSM Image Examiner v3.2 (Carl Zeiss) and Adobe Photoshop v6.0. All measurements were made on three fields per skin section and three skin sections per group ($n = 3$). Vessel density was determined by overlaying three-dimensional reconstructed images of thick sections (100 μm) of skin with a computer-generated delineation of the fluorescent blood vessels. The vessel area density was then calculated and expressed as a percentage of the total area of the section of skin. Vessel numbers were quantified in thin cross-sections (8 μm) and diameters of the largest vertical vessels that run up the length of the reticular layer of the dermis were measured in thick sections (100 μm).

Results

Increased Tie2 Signaling in DT Mice

To examine the consequences of Tie2 overexpression, we have used a previously described binary transgenic system to specifically regulate expression of *Tie2* using a Tie2 promoter.[7,12] Briefly, the tetracycline-responsive transactivator, *tTA*, expressed from the Tie2 promoter (driver transgene) associates with the *tTA* binding site or tetracycline operating sequence (Tet^{OS}) upstream of the *Tie2* cDNA (responder transgene) to allow expression of *Tie2* (Figure 1a). Repression of transgene expression occurs rapidly on administration of a tetracycline analog known as doxycycline. Previous expression analysis of this driver line in early embryos (not shown) and immunostaining for Tie2 and pan endothelial cell (Panec) marker in adult skin indicated that this promoter drives transgene expression in endothelial cells (Figure 1b). However, expression analysis in adult skin revealed that the promoter additionally drives expression in keratinocytes and epithelial cells of the hair follicle (Figure 1; c to e). To further address the potential role for Tie2 in keratinocytes, *Tie2* expression was examined by semiquantitative RT-PCR using RNA extracted from primary mouse (pm) and primary human (ph) KCs. The relative abundance of *Tie2* in pmKCs is low although comparable to that of mouse endothelial cells when normalized to *βActin* levels (Figure 1f). Importantly, both mouse and human keratinocytes do not express the endothelial-specific gene vascular endothelial (*Ve*)-*cadherin*, suggesting that both primary keratinocyte preparations did not possess contaminating endothelial cells. Interestingly, when treated with calcium to induce terminal differentiation, *Tie2* expression is down-regulated in pmKCs (pmKC+) suggesting that Tie2 may play a role in precursor or undifferentiated keratinocytes. Several other mouse cell lines tested also exhibit *Tie2* expression, including preadipocyte, embryonic fibroblast, and neuroblastoma cells (not shown), suggesting an alternative, potentially non-angiogenic role for the receptor in these cell types. Further examination of *Tie2* expression by semiquantitative RT-PCR using RNA extracted from the ear and skin of both WT and DT animals indicates that *Tie2* transgene expression levels are higher in the ear than in the skin (Figure 1g). Accordingly, Tie2 immunoprecipitates of pro-

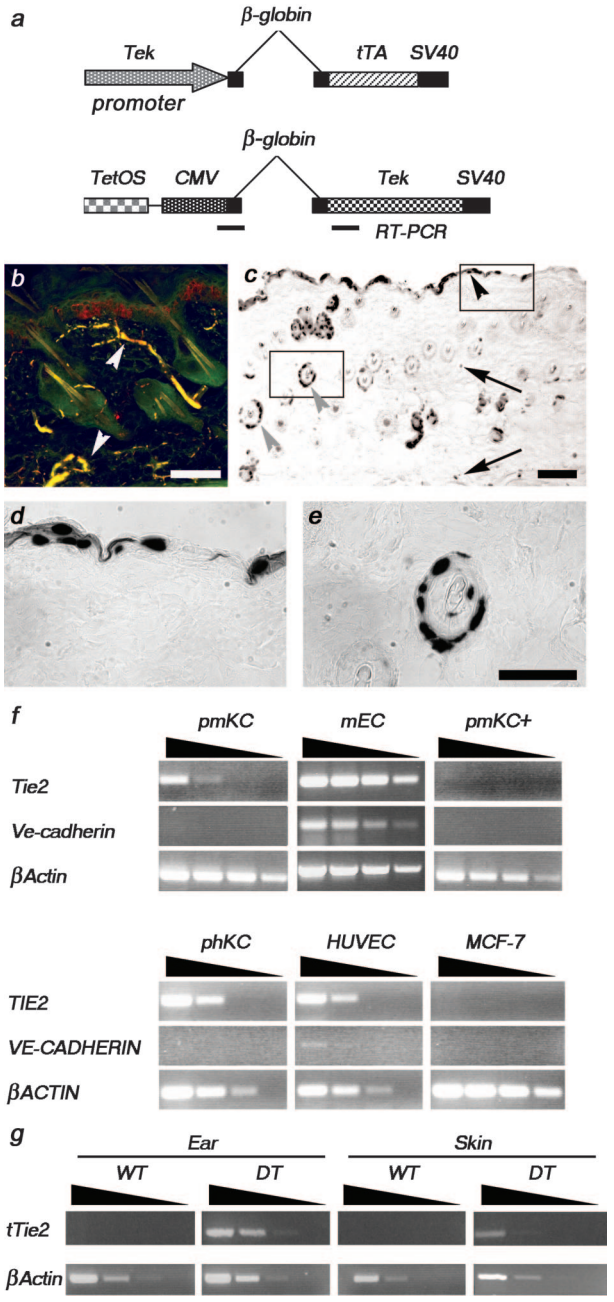

Figure 1. Tie2 expression in DT mice. **a:** Schema of the two transgenes used in these studies to produce the driver line (**top**) and the responder line (**bottom**). **b:** Panec (green) and Tie2 (red) co-staining on a section from adult skin demonstrates co-localization (yellow) of Tie2 with an endothelial cell marker (**white arrowheads**). **c–e:** Analysis of Tie2-driven LacZ expression in the skin of DT mice. Expression of the *nlsLacZ* transgene is seen in endothelial cells (**arrows**), keratinocytes (**black arrowhead**), and epithelial cells of hair follicles (**gray arrowhead**) (**c**). Increased magnification of **insets** in **c** show keratinocytes (**d**) and epithelial cells of hair follicles (**e**). **f:** Semiquantitative RT-PCR analysis of *Tie2* and *Ve-cadherin* expression was completed on RNA isolated from primary mouse (pm) and human (ph) KCs. *Tie2* expression is down-regulated in pmKCs on treatment with calcium (pmKC+). Mouse endothelioma cells and human umbilical vein endothelial cells are positive whereas MCF-7 cells are negative for *Tie2* and *Ve-cadherin* expression. The *βActin* control demonstrates the presence of amplifiable RNA in all samples. cDNA templates were undiluted, diluted 1 in 10, 1 in 100, or 1 in 1000, as illustrated by the wedge. **g:** Semiquantitative RT-PCR analysis of the *Tie2* transgene was performed on RNA isolated from the ear and skin of DT and normal or WT adult mice. Expression of the *Tie2* transgene can be readily detected in the ear and skin of a DT adult mouse. The *βActin* control indicates the presence of amplifiable RNA. cDNA templates were diluted as above. Scale bars, 100 μm.

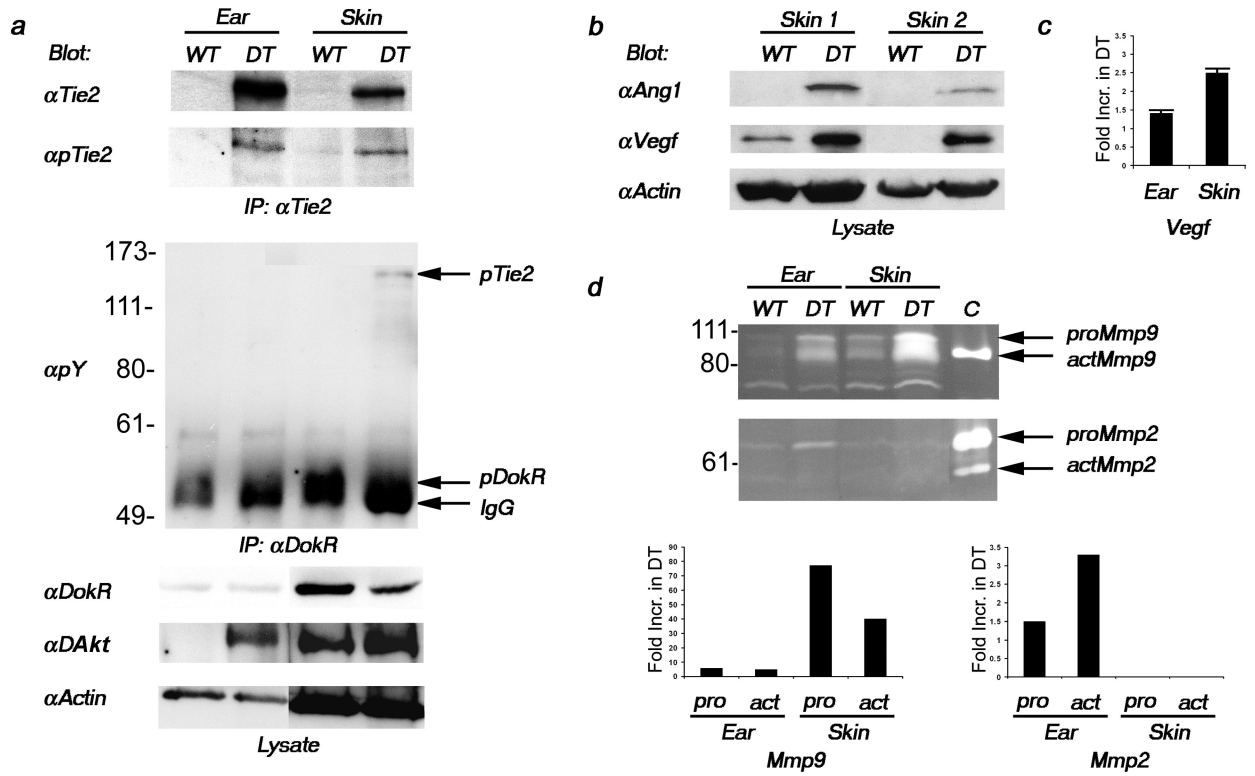

Figure 2. Increased Tie2 expression and signal transduction in DT mice. **a:** Tie2 immunoprecipitates from lysates extracted from the ear and skin of DT and normal (WT) adult mice were immunoblotted with antibodies recognizing phosphorylated Tie2 (pTie2). The blot was then reprobed with anti-Tie2 antibodies. Increased expression and phosphorylation of Tie2 can be observed in DT mice. Lysates were also immunoprecipitated with anti-DokR antibodies and immunoblotted with antibodies recognizing phosphotyrosine (pY). The blot was then reprobed with antibodies recognizing DokR. IgG indicates the position of IgG. Nonimmunoprecipitated lysates (lysate) were incubated with antibodies recognizing either phosphorylated Akt (pAkt) or Actin. **b:** Nonimmunoprecipitated lysates extracted from the skin of two different pairs of DT and WT adult mice were immunoblotted with antibodies recognizing Ang1, Vegf, or Actin. **c:** Vegf protein levels as determined by enzyme-linked immunosorbent assay from lysates prepared from the ear and skin of three different pairs of animals. The fold-increase in Vegf expression in DT over normal mice was determined by densitometry. **d:** Gelatin zymography was performed on lysates prepared from the ear and skin of DT and WT mice. The positions of the 92-kd pro- (proMmp9) and 84- and 82-kd active (actMmp9) forms of Mmp9 are indicated as well as the 72-kd pro- (proMmp2) and 62-kd active (actMmp2) forms of Mmp2. C indicates the position of the positive controls. The fold-increase in Mmp activity in DT over normal mice was determined by densitometry of this representative experiment.

tein lysates prepared from the same mice reveal an approximate 10- to 20-fold increase in Tie2 expression relative to endogenous levels in the skin and ear, respectively, on immunoblotting for Tie2 (Figure 2a). Interestingly, immunoblotting with a phosphorylation state-specific antibody for Tie2 that recognizes phosphorylated tyrosine residues in the carboxy terminal tail of the receptor[21] demonstrates that the receptor is activated in the ear and skin of DT animals (Figure 2a). The presence of the agonistic Tie2 receptor ligand Ang1 in the skin of DT animals supports this observation (Figure 2b) although the potential exists for Ang2 to stimulate Tie2 phosphorylation in this context[22] because *Ang2* mRNA can be weakly detected in the skin of both WT and DT mice (not shown). Activation of the receptor was also measured through the analysis of various signal transduction molecules known to be stimulated downstream of Tie2. Activated thymoma viral proto-oncogene 1 (Akt) [also known as protein kinase B (Pkb)] is present in lysates prepared from both the skin and ear of DT mice and the presence of activated Akt in the skin of WT animals is consistent with the role of Tie2 in transducing an ongoing survival stimulus to endothelial cells through this kinase (Figure 2a).[23] Additionally, phosphorylation of downstream of kinase-related (DokR), a known binding partner and substrate of Tie2,[18] is particularly evident in DokR immunoprecipitates of skin lysates where co-immunoprecipitation of the phosphorylated receptor can also be detected (Figure 2a). Increased secretion and activation of the matrix metalloproteinases (Mmps) Mmp2 and Mmp9 in the ear and skin of DT animals as determined by gelatin zymography is in agreement with recent reports demonstrating that Ang1 signaling can positively regulate their secretion from endothelial cells (Figure 2d).[24] The relationship between Mmp2 and Vegf expression[25–27] as well as the potential for MMP9 to mobilize bound Vegf from the extracellular matrix[28] further prompted us to examine Vegf levels in mice overexpressing Tie2. Immunoblot analysis indicates the presence of Vegf in the skin of DT mice (Figure 2b) and enzyme-linked immunosorbent assay demonstrates 1.4- and 2.5-fold increases in Vegf in the ear and skin, respectively, of DT animals (Figure 2c). Taken together, these biochemical results illustrate an increase in both Tie2 expression and Tie2-signaling intermediates in DT animals; however, because of the expression of Tie2 in keratinocytes, one is unable to unequivocally ascribe all of these activities to the activation of Tie2 in endothelial cells.

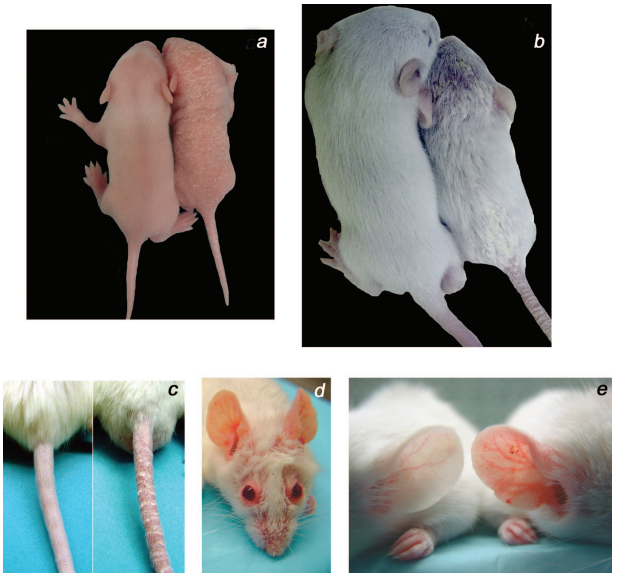

Figure 3. Excess Tie2 expression induces skin abnormalities in DT mice. **a:** A DT mouse (**right**) and a normal (WT) littermate (**left**) at 7 days of age. Erythema and scaling can be observed on the head, back, and tail of the affected mouse. **b:** A DT mouse (**right**) and a normal littermate (**left**) at 2 weeks of age. Note the abnormal appearance of the fur with superficial scaling on the head, lower back, and tail. **c:** Prominent scaling and redness on the tail of a DT mouse (**right**) compared to a normal littermate (**left**) at 2 weeks of age. **d:** A DT adult mouse with prominent redness around the eyes, ears, and snout. **e:** Comparison of ear skin shows increased redness and keratinization on the skin surface of DT mice that is not observed in WT littermates.

Tie2 Overexpression Induces Skin Abnormalities

Several abnormalities are apparent on general inspection of all male and female DT mice when compared with WT littermates. Beginning at approximately postnatal day 5 (P5), the skin of DT neonates is marked by extensive erythema and loosely adherent silver-white scaling (Figure 3a). This skin phenotype persists in older animals in which the emerging hair appears dull and sparse when compared with littermate controls and is covered with focal areas of scaling (Figure 3b) that extend to the tail (Figure 3c). Patches of thickened erythematous skin are particularly noticeable in adult animals around the eyes and snout (Figure 3d) as well as on the ears (Figure 3e) and other extensor surfaces including the knuckles of the legs and nape of the neck (not shown). Although the skin phenotype is fully penetrant, the severity varies in animals within and across litters likely because of the random bred background (CD1) of the mice. More severely affected animals display patchy alopecia (Figure 3, b and d) as well as yellow-brown discoloration of the nails (not shown). There is also an increased genesis of skin lesions at sites of trauma that subsequently become large, thickened, and ulcerated (reminiscent of Koebner phenomenon). Furthermore, DT mice fail to thrive and their sizes are on average 20 to 25% smaller than their WT littermates (Figure 3, a and b). Although complete physiology and pathology screens have revealed no other phenotypic differences between DT and WT mice, older DT animals sporadically develop a white opacity or cloudiness of the eye indicative of an age-related cataract (not shown).

Histological Changes in Skin Lesions of Affected Mice

Histological examination of thin sections of the skin obtained from moderately affected animals demonstrates mild epidermal thickening (hyperplasia) in the skin of the ear, head, and back (Figure 4; b and c, f and g, j and k, respectively) when compared to WT littermates (Figure 4; a, e, and i). More severely affected animals exhibit zones of prominent hyperplasia reflecting regionally variable increases in the number of cell layers in the squamous epithelium (acanthosis) (Figure 4; d, h, and i). Quantitative analysis of the epidermis reveals an increase in epidermal thickness in DT animals approximately three times that seen in WT littermates (Table 1). In some regions of epidermal expansion, uneven elongation of structures resembling rete pegs extend downward into the dermis (Figure 4h) although the density of hair follicles in the mouse skin makes it difficult to rule out the possibility that these structures could also arise as a consequence of altered hair growth in these regions. Serial sections of elongated structures that extend very deep into the dermis demonstrate that these structures encompass hyperplastic hair follicles. The skin of DT mice also includes an increased amount and density of cornified material (compact hyperkeratosis) and areas where nucleated cells are present in the cornified layer (focal parakeratosis). Epidermal alterations in DT mice are accompanied by focal dermal inflammatory infiltrates of mononuclear cells consisting primarily of lymphocytes (Figure 4; f to h) with dispersed macrophages and mast cells. In some areas of skin from severely affected mice, aggregates of neutrophilic polymorphonuclear leukocytes are conspicuous, forming microabscesses within the epidermis (Figure 4f). An increase in the number of blood capillaries with dilated and tortuous changes is also observed in the dermis of DT mice (Figure 4; b to d, f to h, and j to l). The abnormal proximity of blood vessels in the dermal papillae to the overlying parakeratotic scale in regions manifesting thinned epidermis may explain the observed phenomenon of multiple, minute bleeding points when a scale is lifted from the skin (positive Auspitz sign).

Inflammatory Cell Recruitment and Increased Vessel Density in Skin of DT Mice

The inflammatory infiltrate in the skin of DT mice was further characterized immunohistochemically using antibodies specific for the mature T lymphocyte marker CD3 and toluidine blue staining was used to identify basophilic mast cells. As indicated by the purple-stained cells, an apparent increase in the number of dermal mast cells can be seen in the dermis of DT skin when compared to WT littermate skin (Figure 5, a and b). Similarly, CD3-immunoreactive T lymphocytes localize to the dermis and

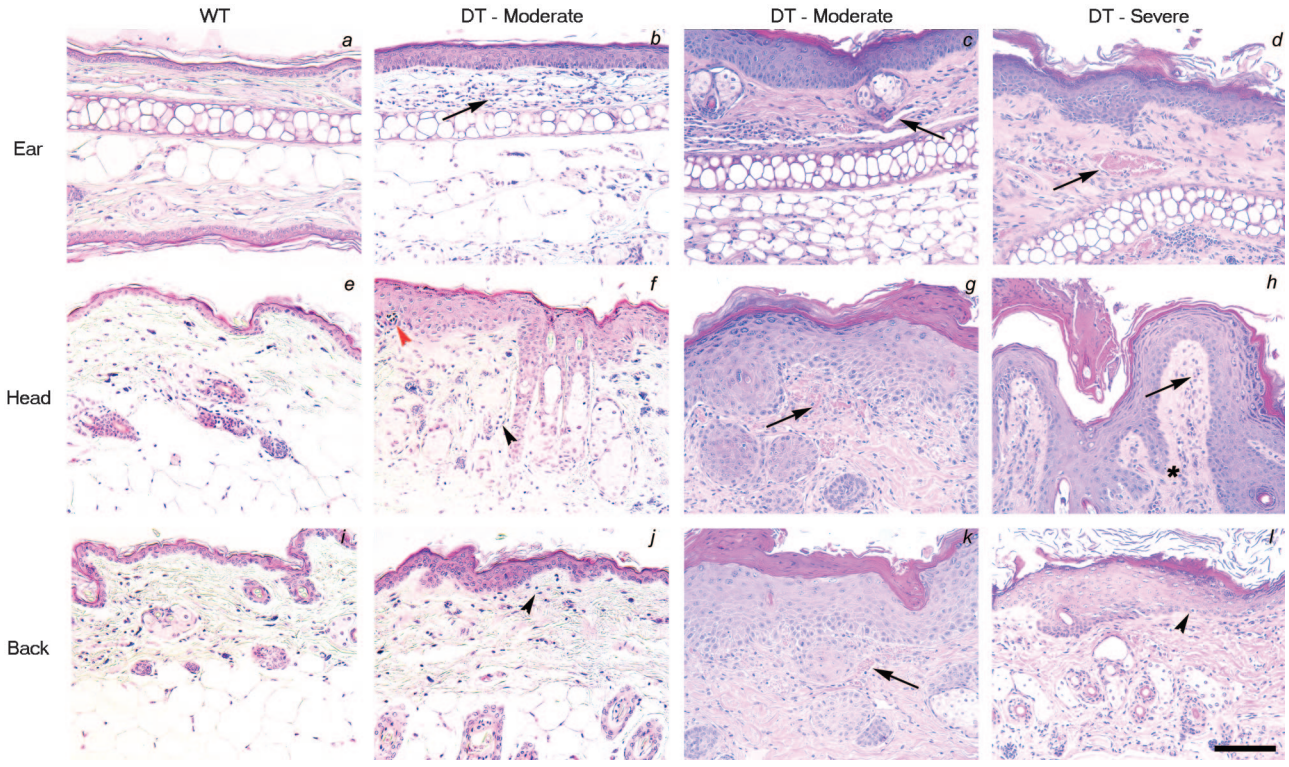

Figure 4. Histological analysis of the skin of DT mice. **a–l:** H&E staining of skin sections from the ear, head, or back of either adult WT mice (**a**, **e**, and **i**), or moderate (**b**, **c**, **f**, **g**, **j**, and **k**) or severely affected (**d**, **h**, and **l**) DT mice. Note the progression in epidermal thickening from moderately affected skin to severely affected skin and the extension of structures resembling rete pegs in the dermis in some regions (**asterisk** in **h**). Also note the increased vessel area density (**arrows**) in DT animals in the dermal papillae with lymphocytic infiltration (**black arrowhead**s). Pockets of neutrophils can also be seen in the cornified layer forming a microabscess (**red arrowhead**) and in other areas throughout the dermis. Scale bar, 50 μm.

epidermis of affected skin while fewer cells are found in WT littermate skin (Figure 5, d and c).

Analysis of pan endothelial cell (Panec) marker (Figure 5, e and f) and platelet and endothelial cell adhesion molecule-1 (Pecam1) (Figure 5, g and h) staining in DT and WT littermates demonstrates larger and more tortuous blood vessels immediately below the epidermis in the skin of DT animals compared to WT littermates (5, e and g). Staining for the myogenic lineage marker smooth muscle actin (Sma) indicates the presence of mesenchymal support cells around vessels in the lower part of the dermis of both WT and DT skin (Figure 5, i and j).

Morphological alterations in the microvasculature can be further visualized by three-dimensional confocal microscopy of fluorescein isothiocyanate-conjugated lectin-perfused animals. Thick sections from these animals were immunohistochemically stained with Sma, Panec, or Pecam1 (not shown) antibodies to visualize smaller vessels closer to the epidermis. Horizontal vessels comprising the subpapillary plexus and deeper cutaneous plexus are larger in DT than WT skin and often extend great distances in close proximity to the hyperproliferative epidermal layer (Figure 6; compare b and c to a, and e and f to d). Additionally, the diameter of vertical vessels that initiate in the subcutaneous tissue and run (up) the length of the reticular layer of the dermis is maintained near the epidermis (Figure 6, b and c). Despite their increased diameter, these vessels remain poorly enveloped by Sma-positive support cells beyond the subcutaneous tissue (Figure 6, b and c). Elongated large lateral microvessels supply the hair follicles and sweat glands of DT skin (Figure 6, e and f); however, in deeper layers of the dermis in regions where such structures are absent, dilated vessels with large lumens reminiscent of mother vessels[29] are observed (Figure 6f). Quantitative analysis of blood vessel area densities, numbers, and diameters in the skin of DT and WT adult animals reveal increased densities and diameters in DT skin compared to WT littermates but no significant change in vessel numbers (Table 1). Taken together, the vascular expansion in Tie2 overexpressing mice appears not to be because of an increased number of vessels or vessel sprouting, but

Table 1. Quantitation of Epidermal Thickness and Blood Vessel Morphology in Wild-Type (WT) and Double-Transgenic (DT) Mice

	Epidermal thickness (μm)	Vessel area density (%)	Vessel number	Vessel diameter (μm)
WT	26.3 ± 6.4	0.09 ± 0.02	28.9 ± 9.1	16.0 ± 3.0
DT	74.1 ± 10.3*	0.24 ± 0.05*	25.2 ± 7.8	33.7 ± 8.9*

*Significantly different from corresponding value for WT mice ($P < 0.05$, Student's *t*-test).

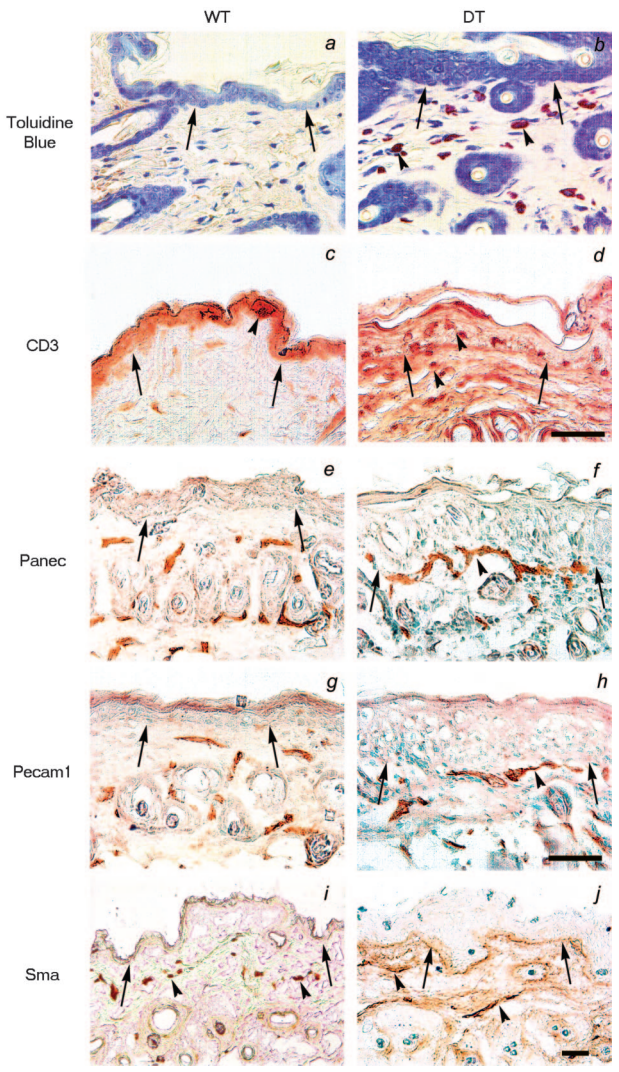

Figure 5. Immunohistological analysis of the skin of DT mice. **a** and **b:** Toluidine blue staining of thin sections reveals infiltration of mast cells (purple staining) throughout the dermis of DT (**b**, **arrowheads**) but not WT mice (**a**). **c** and **d:** Staining of thin sections for the presence of CD3-positive lymphocytes illustrates an apparent increase in T cells in the subepidermal layer of DT mice (**d**, **arrowheads**) compared to WT littermates (**c**). **e–j:** Immunohistochemical staining for Panec, Pecam1, and Sma in skin sections from a DT and WT adult mouse. Staining with the endothelial cell markers Panec (**e** and **f**) and Pecam1 (**g** and **h**) reveals large vessels closer to the epidermis in DT (**f** and **h**, **arrowheads**) compared to WT (**e** and **h**) mice. Sma positivity marks large supported vessels in the deep dermis of both DT and WT skin (**arrowheads** in **i** and **j**). In all sections, the dermo-epidermal junction is indicated with **arrows**. Scale bars: 50 μm (**a–j**); 100 μm (**k** and **l**).

rather because of a consistent and general increase in vessel size.

Tie2 Transgene Expression Is Required to Maintain Skin Alterations in DT Mice

To investigate whether excessive Tie2 expression is required to maintain the skin abnormalities in DT mice, Tie2 transgene expression was repressed in both P7 and adult mice using doxycycline. In the case of the P7 pups, lactating mothers were fed doxycycline in their drinking water to extinguish transgene expression.[7,12] Analysis of Tie2 immunoprecipitates from lysates prepared from ears of DT and WT mice before and after doxycycline treatment demonstrates that the levels of Tie2 from doxycycline-treated DT animals are comparable to those seen in WT littermates, thereby illustrating that repression of the transgene leads to a complete reduction in excess Tie2 production (Figure 7a). Before doxycycline treatment, affected neonates can be readily identified by extensive superficial scaling and reddening of the skin (Figure 7, compare c to b). However, within 4 days of continued administration of doxycycline, DT neonates demonstrate striking improvements in the appearance of the skin and fur and are almost indistinguishable from unaffected WT littermates (Figure 7, compare e to d). Similarly, in adults treated with doxycycline for a period as short as 7 days, the erythematous characteristics of the affected animals before treatment (Figure 7, compare g to f) are markedly improved and the ears in particular become progressively less red (Figure 7, compare i to h). Histological analysis of skin sections obtained from DT or WT littermates both before and after doxycycline treatment clearly demonstrate the transition from a hyperplastic epidermis with prominent inflammation (Figure 7, j and m) to a thinned epidermis resembling the normal counterpart after doxycycline administration (Figure 7, k and n, compared to l and o, respectively). Similarly, blood vessels comprising the papillary and reticular layers of the dermis decrease in diameter and the vessel density appears reduced as vessels become less tortuous (Figure 7, k and n).

Resolution of Tie2-Induced Skin Abnormalities by CsA Treatment

The epidermal abnormalities, leukocytic infiltration, and increased dermal vascularity observed in mouse skin after overexpression of the Tie2 transgene are consistent with the pathology of human psoriasis. To further confirm this, we evaluated the therapeutic response of DT mice to accepted anti-psoriatic treatments. Analysis of Tie2 immunoprecipitates from lysates prepared from the skin of DT and WT mice before and after CsA treatment illustrates that the levels of Tie2 from CsA-treated DT animals remain unchanged comparable to those seen in untreated DT animals; however, the phosphorylation state of the receptor is comparable to that seen in WT and doxycycline-treated DT animals, showing that treatment with CsA leads to a reduction in excess Tie2 activation (Figure 8a). Severely affected adult DT mice were administered systemic CsA and resolution of the skin phenotype (scored by loss of scaling on the tail, increased hair luster, and decreased reddening of the ears and skin around the eyes and snout) was monitored and compared to age-matched DT mice treated with doxycycline. Remarkably, DT animals treated with CsA display a pronounced improvement in the skin phenotype (Figure 8, compare e to d) that is comparable to that seen on initiation of doxycycline treatment in DT mice (Figure 8, compare c to b). Parallel drug treatment of WT mice had no effect on skin morphology or histology (not shown).

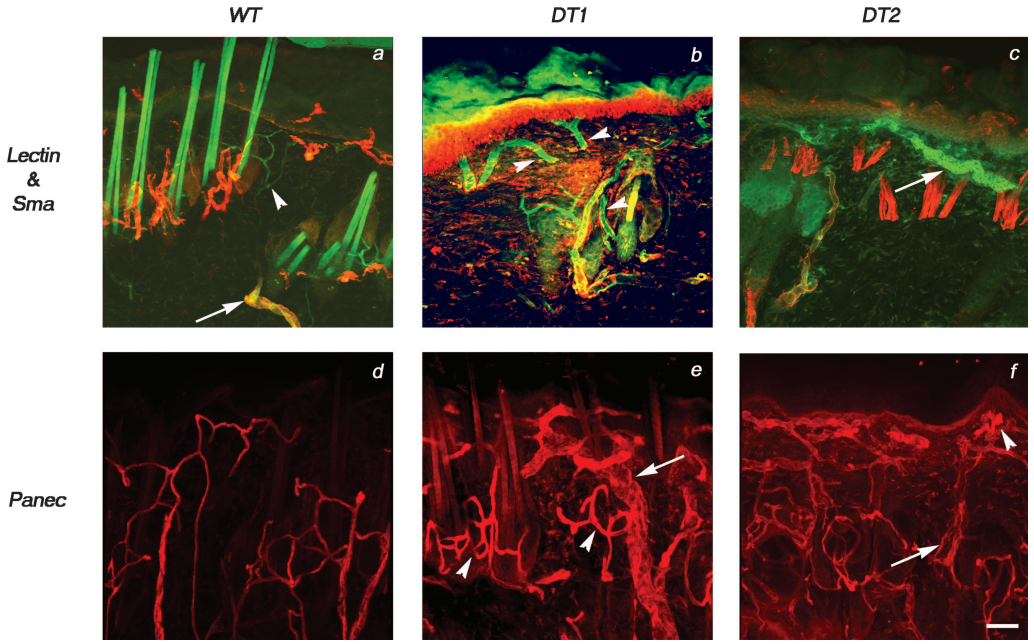

Figure 6. Increased vessel size and tortuousity in DT mice. Thick sections (100 μm) of skin from animals perfused with a fluorescein isothiocyanate-labeled lectin (green) were stained with anti-Sma or anti-Panec antibodies (red) and visualized by confocal microscopy. **a:** Examination of skin from WT mice reveals vertical vessels connecting the cutaneous plexus to the subpapillary plexus that gradually decrease in diameter as they extend toward the epidermis and become progressively less positive for Sma (**arrow**) despite remaining lectin-positive (**arrowhead**). Capillaries in the papillary layer of the dermis of WT mice also stain positive for lectin alone (**arrowhead**). **b** and **c:** Examination of skin from two DT mice reveals large vertical vessels connecting the cutaneous plexus to the subpapillary plexus that do not decrease in diameter toward the epidermis (**arrowheads** in **b**). The indicated vessel also appears to retain increased diameter on bifurcation. The small Sma-negative capillaries below the epidermis of WT skin are replaced by large vessels that remain Sma-negative in DT skin (**arrow** in **c**). **d–f:** The lack of Sma staining within the subpapillary plexus is not because of problems with antibody penetration because similar thick sections stained with Panec demonstrate an intricate vascular bed beneath the epidermis in both WT (**d**) and DT (**e** and **f**) mice. The dermal vasculature of DT skin appears more complex than that of WT skin because vessels stained with Panec are generally of greater diameter (**arrow** in **e**) and appear more tortuous, especially around hair follicles (**arrowheads** in **e**). In addition, vessels with large lumens (**arrow** in **f**) and tangled vessels (**arrowhead** in **f**) can be seen throughout the dermis. Scale bar, 50 μm.

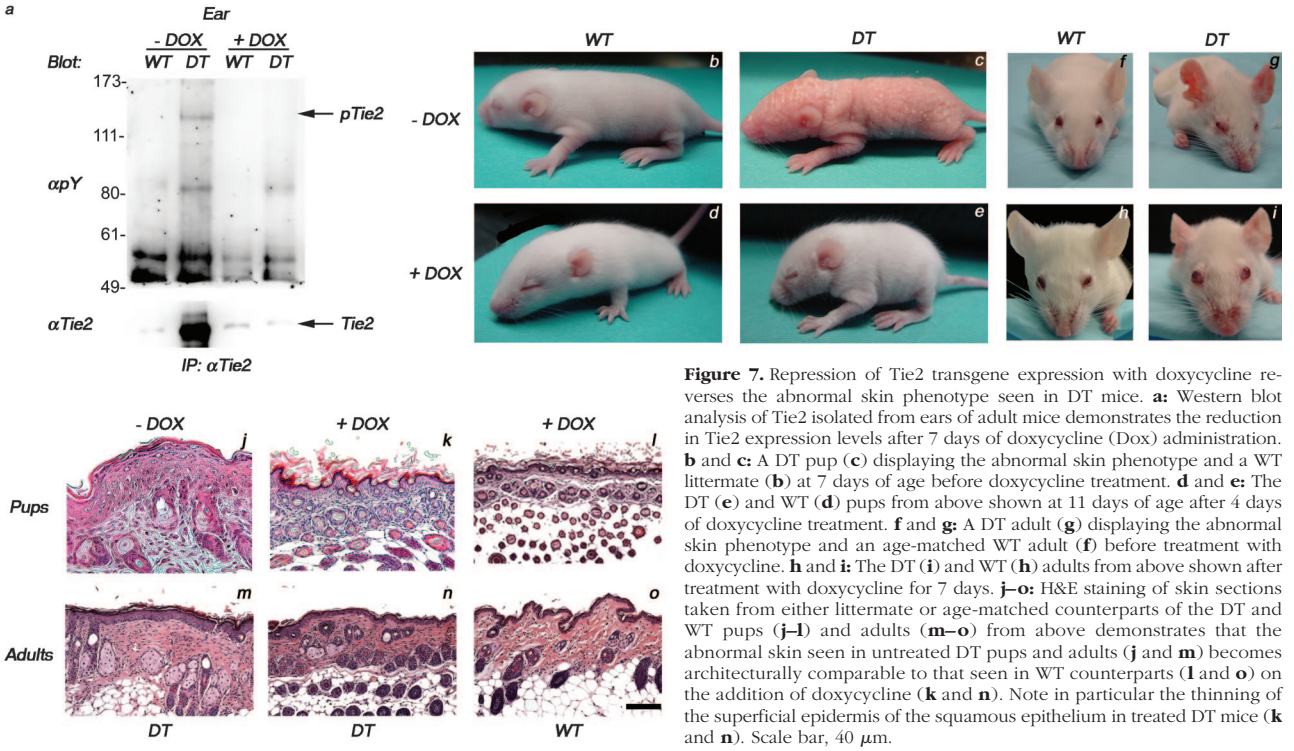

Figure 7. Repression of Tie2 transgene expression with doxycycline reverses the abnormal skin phenotype seen in DT mice. **a:** Western blot analysis of Tie2 isolated from ears of adult mice demonstrates the reduction in Tie2 expression levels after 7 days of doxycycline (Dox) administration. **b** and **c:** A DT pup (**c**) displaying the abnormal skin phenotype and a WT littermate (**b**) at 7 days of age before doxycycline treatment. **d** and **e:** The DT (**e**) and WT (**d**) pups from above shown at 11 days of age after 4 days of doxycycline treatment. **f** and **g:** A DT adult (**g**) displaying the abnormal skin phenotype and an age-matched WT adult (**f**) before treatment with doxycycline. **h** and **i:** The DT (**i**) and WT (**h**) adults from above shown after treatment with doxycycline for 7 days. **j–o:** H&E staining of skin sections taken from either littermate or age-matched counterparts of the DT and WT pups (**j–l**) and adults (**m–o**) from above demonstrates that the abnormal skin seen in untreated DT pups and adults (**j** and **m**) becomes architecturally comparable to that seen in WT counterparts (**l** and **o**) on the addition of doxycycline (**k** and **n**). Note in particular the thinning of the superficial epidermis of the squamous epithelium in treated DT mice (**k** and **n**). Scale bar, 40 μm.

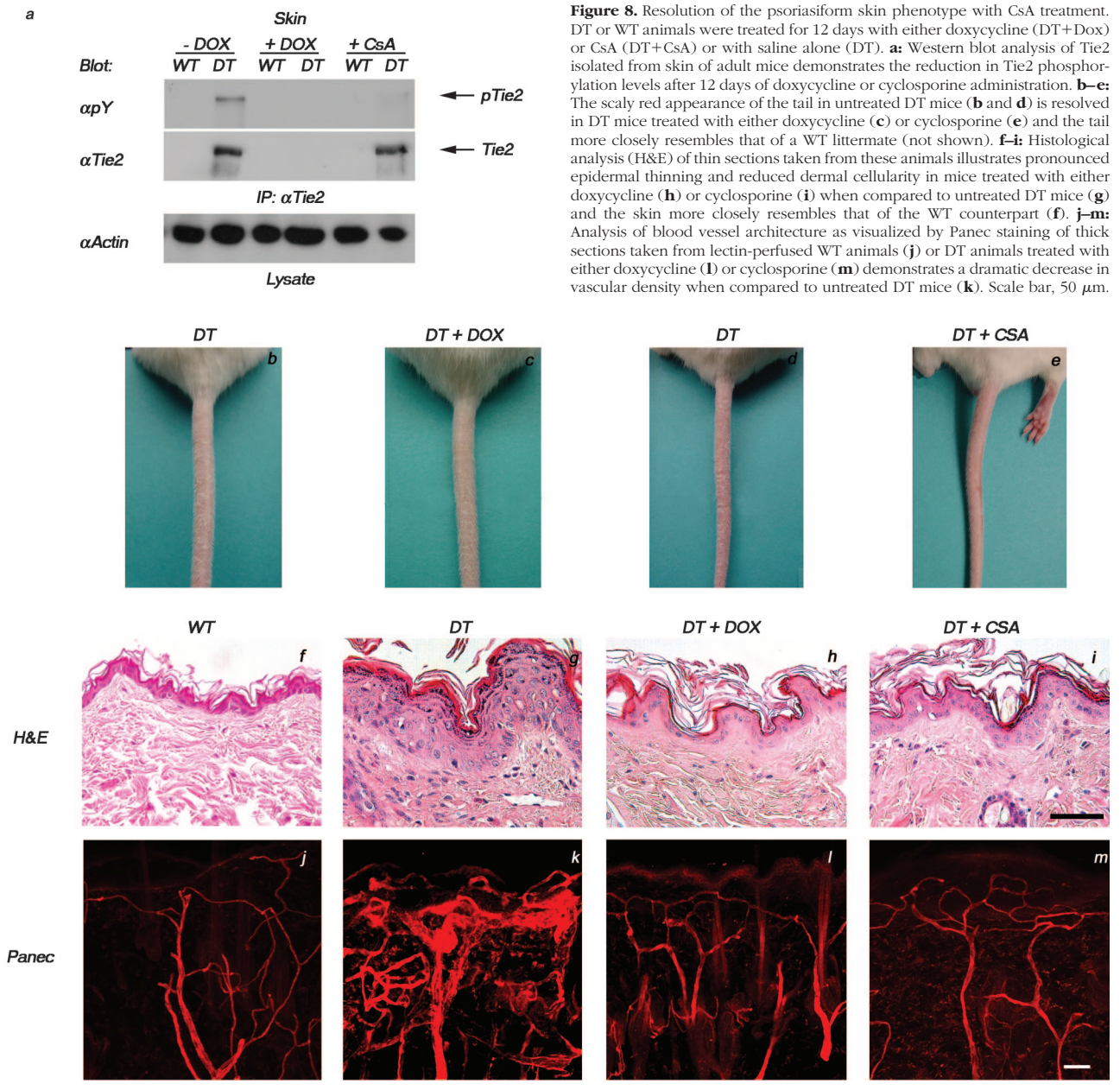

Figure 8. Resolution of the psoriasiform skin phenotype with CsA treatment. DT or WT animals were treated for 12 days with either doxycycline (DT+Dox) or CsA (DT+CsA) or with saline alone (DT). **a:** Western blot analysis of Tie2 isolated from skin of adult mice demonstrates the reduction in Tie2 phosphorylation levels after 12 days of doxycycline or cyclosporine administration. **b–e:** The scaly red appearance of the tail in untreated DT mice (**b** and **d**) is resolved in DT mice treated with either doxycycline (**c**) or cyclosporine (**e**) and the tail more closely resembles that of a WT littermate (not shown). **f–i:** Histological analysis (H&E) of thin sections taken from these animals illustrates pronounced epidermal thinning and reduced dermal cellularity in mice treated with either doxycycline (**h**) or cyclosporine (**i**) when compared to untreated DT mice (**g**) and the skin more closely resembles that of the WT counterpart (**f**). **j–m:** Analysis of blood vessel architecture as visualized by Panec staining of thick sections taken from lectin-perfused WT animals (**j**) or DT animals treated with either doxycycline (**l**) or cyclosporine (**m**) demonstrates a dramatic decrease in vascular density when compared to untreated DT mice (**k**). Scale bar, 50 μm.

Alleviation of the gross skin phenotype (Figure 8, compare h and i to g) is accompanied by histological changes in the skin including epidermal thinning and reduced dermal cellularity and vascular density comparable to that seen in WT mice (Figure 8f). Three-dimensional reconstruction of the vasculature, as visualized by Panec (Figure 8; j to m) and Pecam1 (not shown) immunostaining, demonstrates that blood vessels of CsA-treated DT mice (Figure 8m) are comparable in size and structure to those in doxycycline-treated DT (Figure 8l) and WT mice (Figure 8j). The vessels are generally smaller in diameter than those of untreated DT mice (Figure 8k) and they appear to retract from the epidermis and become less tortuous around hair follicles and sweat glands.

Discussion

The results presented here demonstrate that transgenic expression of *Tie2* in endothelial cells and keratinocytes results in vascular changes reminiscent of those described in human psoriasis. Although known as predominantly an endothelial-specific receptor tyrosine kinase, our finding that *Tie2* is also expressed in keratinocytes is consistent with more recent studies demonstrating *Tie2* expression in other nonendothelial cell types, including hematopoietic stem cells,[30,31] neutrophils,[32] perivascular mesenchymal cells in normal and diseased tissues,[33–36] fibroblast-like cells of choroidal neovascular membranes,[37] and endometrial epithelial and stromal cells.[38] Although the mechanism by which Tie2 signaling in the

epidermis contributes to the manifestation of a psoriasis-like phenotype remains to be determined, it is possible that Tie2 may be mediating its effects in a precursor or stem cell that is able to give rise to differentiated keratinocytes. Such a role for the receptor is suggested by the down-regulation of *Tie2* in primary mouse keratinocytes that have been induced to differentiate on treatment with calcium. Furthermore, the potential for Tie2 to mediate a biological role in epidermal stem cells is supported by recent reports describing an ability for epidermal progenitor cells and transient amplifying cells or follicular stem cells to incorporate into the vasculature of the ischemic limb of a diabetic mouse model or the skin of a wounded mouse recipient, respectively.[39,40]

Previous experiments examining the effects of expression of angiogenic regulators in the skin have determined that although overexpression of Vegf in the epidermis produces abundant tortuous vessels accompanying a psoriasiform skin phenotype,[41–43] epidermal expression of Ang1 results in an increase in vessel number and diameter without the development of psoriatic lesions.[8] The dermal microvasculature in mice overexpressing Tie2 is characterized by an increased number of elongated and dilated capillaries that are tortuous in nature. The composite vascular phenotype observed after Tie2 overexpression suggests that dynamic regulation of the receptor by the angiopoietin family of ligands,[3,4,44] in coordination with other angiogenic modulators including Vegf,[45,46] may be an important factor in the pathogenesis of psoriasis. Activation of Tie2 in the skin here correlates with enhanced expression of the agonistic Tie2 receptor ligand Ang1 and the concomitant rise in Vegf protein may be a result of metalloproteinase action. Importantly, altered expression and activation of Mmp2 and secretion of pro-Mmp9 have previously been detected in human psoriatic epidermis.[47,48]

Morphological changes in the vasculature of mice overexpressing Tie2 are accompanied by altered epidermal proliferation and differentiation as well as leukocytic infiltration characteristic of human psoriasis. Both Ang1 and Ang2 have been shown to be up-regulated with Tie2 in human psoriatic skin lesions and treatment of such lesions correlates with a decrease in expression of Tie2 and its ligands.[10] Accordingly, repression of transgene expression in mice overexpressing Tie2 results in marked mitigation of the skin phenotype. Remarkably, treatment of these mice with immunosuppressive CsA therapy also significantly ameliorates the skin lesions. However, whether resolution is because of the effect of CsA on keratinocyte, endothelial, or immune cells is unknown because it has been shown to directly influence the biology of all three cell types.[43,49,50] These findings collectively indicate a strong interdependency between Tie2-mediated activation of keratinocytes, angiogenesis, and inflammation in the development and maintenance of this psoriasiform phenotype in mice. At present, several engineered and spontaneous animal models of psoriasis exist. Most display various hallmarks of the disease but because of the polygenic nature of psoriasis, these animal models represent only a partial phenocopy of the skin disorder.[51] A recent report by Xia and colleagues[52] describes a transgenic Vegf mouse model of psoriasis in which animals develop numerous features of psoriasis including epidermal, vascular, and inflammatory alterations. This phenotype could be reversed by the treatment of animals with soluble Vegf receptors, illustrating a dependence on Vegf to maintain the phenotype. Whether classic anti-psoriatic therapies showed any efficacy was not reported. Currently, several investigators have developed xenograft models using immunocompromised *scid/scid* recipients that either transfer activated human T cells or graft human psoriatic plaques to mouse skin.[53,54] Although these models provide an excellent representation of the disease, they require access to human tissue samples and are highly complex and technically involved. The spontaneous mouse mutant, flaky skin (*fsn/fsn*), provides a close mouse model of psoriasis as it exhibits many of the key epidermal, vascular, and inflammatory skin alterations[55] but its lack of response to CsA treatment suggests that this phenotype is not immunologically based and consequently hinders its utility in psoriasis research. Thus, the transgenic mice described in this study, which not only develop skin lesions typical of human psoriasis but also respond to CsA, represent a promising new mouse model of psoriasis.

Presently there exists a large body of evidence suggesting that psoriasis is an autoimmune disorder driven by an inflammatory response.[56] Alternatively, it has also been proposed that an initial proliferation of keratinocytes may be the most critical component in the pathogenesis of psoriasis and that inflammation is secondary to this response.[57] Here we present evidence suggesting that the epidermis and vasculature play pivotal roles in the development of a psoriasiform disorder in mice. Although the etiological significance of each of these component responses in psoriasis remains to be clearly defined, the complete dependence on *Tie2* transgene expression to maintain a psoriasis-like phenotype implies that fluctuations in expression of a single modulator may be sufficient for the initiation and/or progression of the diseased state. The unique ability to modulate Tie2 expression levels and monitor pathogenic features of disease progression in this model will provide a useful biological tool for the development and testing of novel molecular anti-psoriatic therapies. Moreover, breeding experiments with the vast array of engineered mouse mutants that affect various aspects of keratinocyte, endothelial, or immune cell biology may provide further insight into the role of each of these cell types in the manifestation of psoriasis.

Acknowledgments

We thank Dr. Andrew Brooks (University of Guelph, Guelph, Ontario, Canada) and Dr. Venita Jay (Hospital for Sick Children, Toronto, Ontario, Canada) for helpful discussions and technical advice, Dr. Mike Conner (Sunnybrook and Women's Research Institute, Toronto, Ontario) for MCF-7 cells, Sue Farinaccio for her excellent administrative assistance, and Laura Kaufer for technical assistance.

References

1. Dumont DJ, Gradwohl G, Fong GH, Puri MC, Gertsenstein M, Auerbach A, Breitman ML: Dominant-negative and targeted null mutations in the endothelial receptor tyrosine kinase, tek, reveal a critical role in vasculogenesis of the embryo. Genes Dev 1994, 8:1897–1909
2. Sato TN, Tozawa Y, Deutsch U, Wolburg-Buchholz K, Fujiwara Y, Gendron-Maguire M, Gridley T, Wolburg H, Risau W, Qin Y: Distinct roles of the receptor tyrosine kinases Tie-1 and Tie-2 in blood vessel formation. Nature 1995, 376:70–74
3. Suri C, Jones PF, Patan S, Bartunkova S, Maisonpierre PC, Davis S, Sato TN, Yancopoulos GD: Requisite role of angiopoietin-1, a ligand for the TIE2 receptor, during embryonic angiogenesis. Cell 1996, 87:1171–1180
4. Maisonpierre PC, Suri C, Jones PF, Bartunkova S, Wiegand SJ, Radziejewski C, Compton D, McClain J, Aldrich TH, Papadopoulos N, Daly TJ, Davis S, Sato TN, Yancopoulos GD: Angiopoietin-2, a natural antagonist for Tie2 that disrupts in vivo angiogenesis. Science 1997, 277:55–60
5. Ward N, Dumont DJ: The angiopoietins and Tie2/Tek: adding to the complexity of cardiovascular development. Semin Cell Dev Biol 2002, 1:19–27
6. Puri MC, Partanen J, Rossant J, Bernstein A: Interaction of the TEK and TIE receptor tyrosine kinases during cardiovascular development. Development 1999, 126:4569–4580
7. Jones N, Voskas D, Master Z, Sarao R, Jones J, Dumont DJ: Rescue of the early vascular defects in Tek/Tie2 null mice reveals an essential survival function. EMBO Rep 2001, 2:438–445
8. Suri C, McClain J, Thurston G, McDonald DM, Zhou H, Oldmixon EH, Sato TN, Yancopoulos GD: Increased vascularization in mice overexpressing angiopoietin-1. Science 1998, 282:468–471
9. Vikkula M, Boon LM, Carraway KL, Calvert JT, Diamonti AJ, Goumnerov B, Pasyk KA, Marchuk DA, Warman ML, Cantley LC, Mulliken JB, Olsen BR: Vascular dysmorphogenesis caused by an activating mutation in the receptor tyrosine kinase TIE2. Cell 1996, 87:1181–1190
10. Kuroda K, Sapadin A, Shoji T, Fleischmajer R, Lebwohl M: Altered expression of angiopoietins and Tie2 endothelium receptor in psoriasis. J Invest Dermatol 2001, 116:713–720
11. Braverman IM: The cutaneous microcirculation. J Invest Dermatol Symp Proc 2000, 5:3–9
12. Sarao R, Dumont DJ: Conditional transgene expression in endothelial cells. Transgenic Res 1998, 7:421–427
13. D'Souza SJ, Pajak A, Balazsi K, Dagnino L: Ca2+ and BMP-6 signaling regulate E2F during epidermal keratinocyte differentiation. J Biol Chem 2001, 276:23531–23538
14. Boyce ST, Ham RG: Cultivation, frozen storage and clonal growth of normal human epidermal keratinocytes in serum free media. J Tissue Culture Methods 1985, 9:83–93
15. Fiedler U, Krissl T, Koidl S, Weiss C, Koblizek T, Deutsch U, Martiny-Baron G, Marme D, Augustin HG: Angiopoietin-1 and angiopoietin-2 share the same binding domains in the Tie-2 receptor involving the first Ig-like loop and the epidermal growth factor-like repeats. J Biol Chem 2003, 278:1721–1727
16. Gill M, Dias S, Hattori K, Rivera ML, Hicklin D, Witte L, Girardi L, Yurt R, Himel H, Rafii S: Vascular trauma induces rapid but transient mobilization of VEGFR2(+)AC133(+) endothelial precursor cells. Circ Res 2001, 88:167–174
17. Gory-Faure S, Prandini MH, Pointu H, Roullot V, Pignot-Paintrand I, Vernet M, Huber P: Role of vascular endothelial-cadherin in vascular morphogenesis. Development 1999, 10:2093–2102
18. Jones N, Dumont DJ: The Tek/Tie2 receptor signals through a novel Dok-related docking protein, Dok-R. Oncogene 1998, 17:1097–1108
19. Elson DA, Thurston G, Huang LE, Ginzinger DG, McDonald DM, Johnson RS, Arbeit JM: Induction of hypervascularity without leakage or inflammation in transgenic mice overexpressing hypoxia-inducible factor-1alpha. Genes Dev 2001, 15:520–532
20. Yano M, Iwama A, Nishio H, Suda J, Takada G, Suda T: Expression and function of murine receptor tyrosine kinases, TIE and TEK, in hematopoietic stem cells. Blood 1997, 89:4317–4326
21. Jones N, Chen SH, Sturk C, Master Z, Tran J, Kerbel RS, Dumont DJ: A unique autophosphorylation site on Tie2/Tek mediates Dok-R phosphotyrosine binding domain binding and function. Mol Cell Biol 2003, 23:2658–2668
22. Teichert-Kuliszewska K, Maisonpierre PC, Jones N, Campbell AI, Master Z, Bendeck MP, Alitalo K, Dumont DJ, Yancopoulos GD, Stewart DJ: Biological action of angiopoietin-2 in a fibrin matrix model of angiogenesis is associated with activation of Tie2. Cardiovasc Res 2001, 49:659–670
23. Kim I, Kim HG, So J-N, Kim JH, Kwak HJ, Koh GY: Angiopoietin-1 regulates endothelial cell survival through the phosphatidylinositol 3′-kinase/Akt signal transduction pathway. Circ Res 2000, 86:24–29
24. Kim I, Kim HG, Moon SO, Chae SW, So JN, Koh KN, Ahn BC, Koh GY: Angiopoietin-1 induces endothelial cell sprouting through the activation of focal adhesion kinase and plasmin secretion. Circ Res 2000, 86:952–959
25. Hajitou A, Sounni NE, Devy L, Grignet-Debrus C, Lewalle JM, Li H, Deroanne CF, Lu H, Colige A, Nusgens BV, Frankenne F, Maron A, Yeh P, Perricaudet M, Chang Y, Soria C, Calberg-Bacq CM, Foidart JM, Noel A: Down-regulation of vascular endothelial growth factor by tissue inhibitor of metalloproteinase-2: effect on in vivo mammary tumor growth and angiogenesis. Cancer Res 2001, 61:3450–3457
26. Deryugina EI, Soroceanu L, Strongin AY: Up-regulation of vascular endothelial growth factor by membrane-type 1 matrix metalloproteinase stimulates human glioma xenograft growth and angiogenesis. Cancer Res 2002, 62:580–588
27. Sounni NE, Devy L, Hajitou A, Frankenne F, Munaut C, Gilles C, Deroanne C, Thompson EW, Foidart JM, Noel A: MT1-MMP expression promotes tumor growth and angiogenesis through an up-regulation of vascular endothelial growth factor expression. FASEB J 2002, 16:555–564
28. Bergers G, Brekken R, McMahon G, Vu TH, Itoh T, Tamaki K, Tanzawa K, Thorpe P, Itohara S, Werb Z, Hanahan D: Matrix metalloproteinase-9 triggers the angiogenic switch during carcinogenesis. Nat Cell Biol 2000, 2:737–744
29. Pettersson A, Nagy JA, Brown LF, Sundberg C, Morgan E, Jungles S, Carter R, Krieger JE, Manseau EJ, Harvey VS, Eckelhoefer IA, Feng D, Dvorak AM, Mulligan RC, Dvorak HF: Heterogeneity of the angiogenic response induced in different normal adult tissues by vascular permeability factor/vascular endothelial growth factor. Lab Invest 2000, 80:99–115
30. Hattori K, Dias S, Heissig B, Hackett NR, Lyden D, Tateno M, Hicklin DJ, Zhu Z, Witte L, Crystal RG, Moore MA, Rafii S: Vascular endothelial growth factor and angiopoietin-1 stimulate postnatal hematopoiesis by recruitment of vasculogenic and hematopoietic stem cells. J Exp Med 2001, 193:1005–1014
31. Takakura N, Huang XL, Naruse T, Hamaguchi T, Dumont DJ, Yancopoulos GD, Suda T: Critical role of the Tie2 endothelial receptor in the development of definitive hematopoiesis. Immunity 1998, 9:677–686
32. Lemieux C, Maliba R, Favier J, Theoret JF, Merhi Y, Sirois MG: Angiopoietins can directly activate endothelial cells and neutrophils to promote proinflammatory responses. Blood (in press)
33. Iurlaro M, Scatena M, Zhu WH, Fogel E, Wieting SL, Nicosia RF: Rat aorta-derived mural precursor cells express the Tie2 receptor and respond directly to stimulation by angiopoietins. J Cell Sci 2003, 116:3635–3643
34. Tian S, Hayes AJ, Metheny-Barlow LJ, Li LY: Stabilization of breast cancer zenograft tumour neovasculature by angiopoietin-1. Br J Cancer 2002, 86:645–651
35. Shahrara S, Volin MV, Connors MA, Haines KG, Koch AE: Differential expression of the angiogenic Tie receptor family in arthritic and normal synovial tissue. Arthritis Res 2002, 4:201–208
36. Calvert JT, Riney TJ, Kontos CD, Cha EH, Prieto VG, Shea RC, Berg JN, Nevin NC, Simpson SA, Pasyk KA, Speer MC, Peters KG, Marchuk DA: Allelic and locus heterogeneity in inherited venous malformations. Hum Mol Genet 1999, 8:1279–1289
37. Otani A, Takagi H, Oh H, Koyama S, Matsumura M, Honda Y: Expression of angiopoietins and Tie2 in human choroidal neovascular membranes. Invest Ophthalmol Vis Sci 1999, 40:1912–1920
38. Hirchenhain J, Huse I, Hess A, Bielfeld P, De Bruyne F, Krussel JS: Differential expression of angiopoietins 1 and 2 and their receptor Tie-2 in human endometrium. Mol Hum Reprod 2003, 9:663–669
39. Jiao C, Bronner S, Mercer KL, Sheriff DD, Schatteman GC, Dunnwald M: Epidermal cells accelerate the restoration of the blood flow in diabetic ischemic limbs. J Cell Sci 2004, 117:1055–1063
40. Amoh Y, Li L, Yang M, Moossa AR, Katsuoka K, Penman S, Hoffman RM: Nascent blood vessels in the skin arise from nestin-expressing hair-follicle cells. Proc Natl Acad Sci USA 2004, 101:13291–13295

41. Detmar M, Brown LF, Schon MP, Elicker BM, Velasco P, Richard L, Fukumura D, Monsky W, Claffey KP, Jain RK: Increased microvascular density and enhanced leukocyte rolling and adhesion in the skin of VEGF transgenic mice. J Invest Dermatol 1998, 111:1–6
42. Bhushan M, McLaughlin B, Weiss JB, Griffiths CE: Levels of endothelial cell stimulating angiogenesis factor and vascular endothelial growth factor are elevated in psoriasis. Br J Dermatol 1999, 141: 1054–1060
43. Hernández GL, Volpert OV, Íñiguez MA, Lorenzo E, Martínez-Martínez S, Grau R, Fresno M, Redondo JM: Selective inhibition of vascular endothelial growth factor-mediated angiogenesis by cyclosporin A: roles of the nuclear factor of activated T cells and cyclooxygenase 2. J Exp Med 2001, 193:607–620
44. Valenzuela DM, Griffiths JA, Rojas J, Aldrich TH, Jones PF, Zhou H, McClain J, Copeland NG, Gilbert DJ, Jenkins NA, Huang T, Papadopoulos N, Maisonpierre PC, Davis S, Yancopoulos GD: Angiopoietins 3 and 4: diverging gene counterparts in mice and humans. Proc Natl Acad Sci USA 1999, 96:1904–1909
45. Thurston G, Suri C, Smith K, McClain J, Sato TN, Yancopoulos GD, McDonald DM: Leakage-resistant blood vessels in mice transgenically overexpressing angiopoietin-1. Science 1999, 286:2511–2514
46. Asahara T, Chen D, Takahashi T, Fujikawa K, Kearney M, Magner M, Yancopoulos GD, Isner JM: Tie2 receptor ligands, angiopoietin-1 and angiopoietin-2, modulate VEGF-induced postnatal neovascularization. Circ Res 1998, 83:233–240
47. Fleischmajer R, Kuroda K, Hazan R, Gordon RE, Lebwohl MG, Sapadin AN, Unda F, Iehara N, Yamada Y: Basement membrane alterations in psoriasis are accompanied by epidermal overexpression of MMP-2 and its inhibitor TIMP-2. J Invest Dermatol 2001, 115:771–777
48. Suomela S, Kariniemi AL, Snellman E, Saarialho-Kere U: Metalloelastase (MMP-12) and 92-kDa gelatinase (MMP-9) as well as their inhibitors, TIMP-1 and -3, are expressed in psoriatic lesions. Exp Dermatol 2001, 10:175–183
49. Nickoloff BJ, Fisher GJ, Mitra RS, Voorhees JJ: Additive and synergistic antiproliferative effects of cyclosporin A and gamma interferon on cultured human keratinocytes. Am J Pathol 1988, 131:12–18
50. Rao A, Luo C, Hogan PG: Transcription factors of the NFAT family: regulation and function. Annu Rev Immunol 1997, 15:707–747
51. Schon MP: Animal models of psoriasis—what can we learn from them? J Invest Dermatol 1999, 112:405–410
52. Xia YP, Li B, Hylton D, Detmar M, Yancopoulos GD, Rudge JS: Transgenic delivery of VEGF to the mouse skin leads to an inflammatory condition resembling human psoriasis. Blood 2003, 102: 161–168
53. Schon MP, Detmar M, Parker CM: Murine psoriasis-like disorder induced by naive CD4+ T cells. Nat Med 1997, 3:183–188
54. Nickoloff BJ, Kunkel SL, Burdick M, Strieter RM: Severe combined immunodeficiency mouse and human psoriatic skin chimeras. Validation of a new animal model. Am J Pathol 1995, 146:580–588
55. Sundberg JP, France M, Boggess D, Sundberg BA, Jenson AB, Beamer WG, Shultz LD: Development and progression of psoriasiform dermatitis and systemic lesions in the flaky skin (fsn) mouse mutant. Pathobiology 1997, 65:271–286
56. Nickoloff BJ: The immunologic and genetic basis of psoriasis. Arch Dermatol 1999, 135:1104–1110
57. Werner S, Smola H: Paracrine regulation of keratinocyte proliferation and differentiation. Trends Cell Biol 2001, 11:143–146